THE JOURNAL OF BIOLOGICAL CHEMISTRY
© 1995 by The American Society for Biochemistry and Molecular Biology, Inc.

Vol. 270, No. 18, Issue of May 5, pp. 10514–10524, 1995
*Printed in U.S.A.*

# A $Ca^{2+}$-binding Chimera of Human Lysozyme and Bovine α-Lactalbumin That Can Form a Molten Globule*

(Received for publication, November 17, 1994, and in revised form, February 8, 1995)

**Els Pardon‡, Petra Haezebrouck§, Annie De Baetselier¶, Shaun D. Hooke‖, Katherine T. Fancourt‖, Johan Desmet, Christopher M. Dobson‖**, Herman Van Dael, and Marcel Joniau‡‡**

*From the Interdisciplinary Research Center, K. U. Leuven, Campus Kortrijk, B 8500 Kortrijk, Belgium, the ‖Oxford Center for Molecular Sciences, New Chemistry Laboratory, University of Oxford, Oxford OX1 3QT, United Kingdom, and ¶Innogenetics, Industriepark Zwijnaarde 7B4, B 9052 Gent, Belgium*

**In contrast to lysozymes, which undergo two-state thermal denaturation, the $Ca^{2+}$-free form of the homologous α-lactalbumins forms an intermediate "molten globule" state. To understand this difference, we have produced a chimera of human lysozyme and bovine α-lactalbumin. In the synthetic gene of the former the sequence coding for amino acid residues 76–102 was replaced by that for bovine α-lactalbumin 72–97, which represents the $Ca^{2+}$-binding loop and the central helix C. The chimeric protein, LYLA1, expressed in *Saccharomyces cerevisiae* was homogeneous on electrophoresis and mass spectrometry. Its $Ca^{2+}$ binding constant was 2.50 (±0.04) × $10^8$ $M^{-1}$, and its muramidase activity 10% of that of human lysozyme. One-dimensional NMR spectroscopy indicated the presence of a compact, well structured protein. From two-dimensional NMR spectra, main chain resonances for 118 of a total of 129 residues could be readily assigned. Nuclear Overhauser effect analysis and hydrogen-deuterium exchange measurements indicated the presence and persistence of all expected secondary structure elements. Thermal denaturation, measured by circular dichroism, showed a single transition temperature for the $Ca^{2+}$ form at 90 °C, whereas unfolding of the apo form occurred at 73 °C in the near-UV and 81 °C in the far-UV range. These observations illustrate that by transplanting the central part of bovine α-lactalbumin, we have introduced into human lysozyme two important properties of α-lactalbumins, *i.e.* stabilization through $Ca^{2+}$ binding and molten globule behavior.**

Chicken-type (c-type) lysozymes and α-lactalbumins are evolutionarily related proteins (1). Their comparative study offers interesting possibilities in the fields of protein folding (2–4) and enzymatic functioning. Although their amino acid sequences (5) and three-dimensional structures (6, 7) are largely homologous, functionally they are widely different. Lysozymes catalyze the hydrolysis of the β1–4 glycosidic linkage between *N*-acetylglucosamine and *N*-acetylmuramic acid in the main polysaccharide constituent of Gram-positive bacterial cell walls. Their hydrolytic activity is carried by two essential carboxylate groups, contributed in human lysozyme by residues Glu-35 and Asp-53.[1] On the other hand, α-lactalbumins regulate lactose biosynthesis by modulating the specificity of β-galactosyltransferase. One of the best characterized functions of α-lactalbumins is their ability to bind $Ca^{2+}$ strongly. This property resides in a typical $Ca^{2+}$-binding loop, in which two peptide carbonyls and three carboxylate groups (Asp-82, Asp-87 and Asp-88 in the bovine species) act as ligands (8). The binding of $Ca^{2+}$ to α-lactalbumin results in the formation of a stable metalloprotein. Dissociation of $Ca^{2+}$, extremes of pH, elevated temperatures, or moderate concentrations of denaturant lead to the appearance of a typical partially unfolded state (9), which has been designated a molten globule state. It has been characterized by a variety of measurements and shown to exhibit a high content of secondary structure, considerable compactness, nonspecific tertiary structure and significant structural flexibility (10–12). As a result, upon denaturation molecules of α-lactalbumin pass in a multistate process from a native folded state through an equilibrium molten globule intermediate into a completely unfolded state. By contrast, lysozymes generally conform to the classical two-state model for cooperative unfolding without showing an intermediate state with molten globule character. We have recently observed a partially unfolded state comparable with the molten globule state of α-lactalbumin in the case of equine lysozyme (13). It is indicative that, although most lysozymes are unable to bind $Ca^{2+}$, equine lysozyme possesses a $Ca^{2+}$-binding loop (14).

Protein engineering experiments mostly involve the introduction of point mutations at specific sites into well characterized enzymes in order to investigate the role of the corresponding amino acid residues either in binding and catalysis or in molecular structure and stability. Since the stability of protein molecules can be considerably promoted by the introduction of metal ion binding sites, several attempts have been made to introduce the $Ca^{2+}$ binding function of α-lactalbumin in lysozyme by site-directed mutagenesis. Kuroki *et al.* (15) have shown that introducing two of the necessary Asp residues at the corresponding sites in the human lysozyme molecule results in a functional $Ca^{2+}$-binding site. More recently, we have

* This work was supported by grants from the Belgian Fonds voor Geneeskundig Wetenschappelijk Onderzoek and the Research Council of the K. U. Leuven. The Oxford Center for Molecular Sciences is funded jointly by the Engineering and Physical Sciences Research Council, Biotechnology and Biological Sciences Research Council, and Medical Research Council. The costs of publication of this article were defrayed in part by the payment of page charges. This article must therefore be hereby marked "*advertisement*" in accordance with 18 U.S.C. Section 1734 solely to indicate this fact.

‡ Supported by a grant from the Instituut voor Wetenschap en Technologie of the Flemish Community.

§ Grantee of the Research Council of the K. U. Leuven.

** Supported in part by an International Research Scholars award from the Howard Hughes Medical Foundation and by a Leverhulme Trust Senior Research Fellowship from the Royal Society.

‡‡ To whom correspondence should be addressed: Interdisciplinary Research Center, K. U. Leuven Campus Kortrijk, Belgium. Tel.: 32-56-24-61-11; Fax: 32-56-24-69-97.

[1] As a rule, the amino acid sequence numbering used refers to HLY, unless otherwise stated.

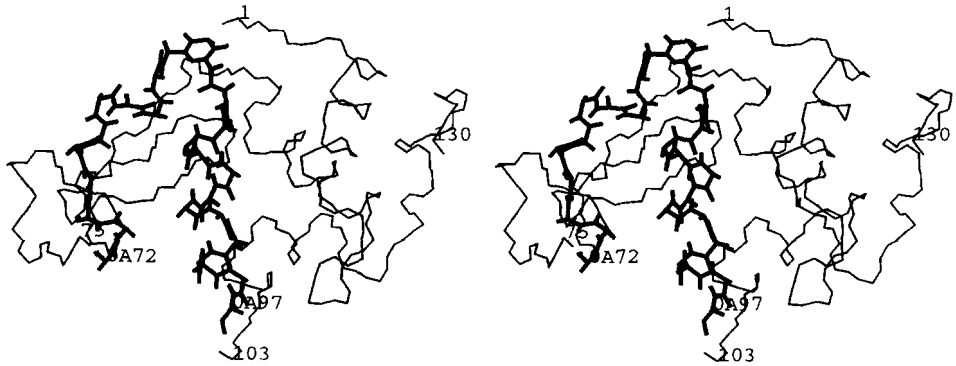


FIG. 1. **Model of the constitutive parts of LYLA1.** Starting from the atomic coordinates of HLY (Brookhaven Data Bank code 1LZ1) and those of BLA, derived from the baboon lactalbumin data (BDB 1 ALC) by conservative on-screen mutation, the chimeric protein was modeled. The transplanted BLA sequence (termed OA72-OA97 and shown in *bold* on the figure) was optimally fitted to the homologous HLY sequence 76–102. As a result, the BLA-derived residue OA72 is within binding distance of the HLY acceptor site 75. However, between BLA residue OA97 and HLY residue 103 a small gap exists, due to deletion of Arg-101. The possible consequences of this deletion are discussed in the text.

been able to demonstrate, first, that a single Asp (A92D) suffices for $Ca^{2+}$ binding and, second, that another mutant (M4[2]) which contains a fully equipped $Ca^{2+}$ site is clearly stabilized against thermal denaturation in its $Ca^{2+}$-bound form (16). In the meantime, the latter mutant was found to display molten globule characteristics at very low pH (17).

In the present contribution we describe a chimera, LYLA1, obtained by transplanting the central segment of bovine α-lactalbumin, which comprises the $Ca^{2+}$-binding loop and the main helix C, into the homologous position in human lysozyme. The result is a compact, well structured molecule, which has the ability to undergo $Ca^{2+}$-induced conformational changes and which shows the typical multistate unfolding behavior of α-lactalbumin.

## EXPERIMENTAL PROCEDURES

*Materials*—Restriction enzymes were purchased from Boehringer Mannheim and from New England Biolabs. Oligonucleotides needed for site-directed mutagenesis were obtained from Pharmacia Biotech Inc. and from the Laboratory of Genetics (University of Ghent, Belgium). *Micrococcus luteus* cells were from Boehringer; *N,N′,N″*-triacetylchitotriose, $(GlcNAc)_3$, came from Sigma; Fura-2 was a product of Molecular Probes.

Natural human lysozyme (HLY), isolated from human milk, was obtained from U. S. Biochemical Corp. Recombinant (wild-type) human lysozyme (rHLY) was expressed in *Saccharomyces cerevisiae* from a synthetic gene and purified as described (18, 19). The HLY mutant, in which a functional $Ca^{2+}$-binding site was introduced by site-directed mutagenesis of four different amino acid residues (M4), has been described before (16). Natural bovine α-lactalbumin (BLA) isolated from cows' milk was obtained from Sigma.

*Strains and Media—Escherichia coli* cells DH5α (*supE44 ΔlacU169 (ϕ80laczΔM15) hsdR17 endA1 recA1 gyrA96 thi-1 relA1*), CJ236 (*dut-1 ung-1 thi-1 relA1*, pCJ105($Cm^r$)), and MV1190 (*Δlac-proAB thi supE (Δscr1-recA)306*::Tn10($tet^r$) (F′ *traD36 proAB, lacI$^q$Z ΔM15*)) were used as host strains for bacterial transformations and routine plasmid preparations. They were grown in Luria broth containing 1% Bacto-tryptone, 0.5% Bacto-yeast extract and 1% NaCl (optionally with 1.5% Bacto-agar).

*S. cerevisiae* GRF182 (α, leu2–3, leu2–112, his3–11, his3–15, ura3Δ, pep4Δ, CAN, cir°), a derivative of GRF18 (20) was used as the host strain and was cultivated either in uracil- or leucine-selective medium (with 8% sucrose added) or in YPD medium (8% sucrose) buffered with 50 mM MES, pH 7 (21).

*Plasmids*—Plasmid pTZ18U was obtained from Bio-Rad. Plasmid pTZs31T, which carries the synthetic bovine α-lactalbumin gene after the triose phosphate isomerase promotor, is a derivative of pSCMFs-BLA (21). In this construct the original codon at position 30:GCG, coding for Ala due to a misinterpretation of the data of Vilotte *et al.* (22) on the cDNA sequence of the *bla* gene, was corrected by site-directed mutagenesis to ACG, coding for Thr (23).

Plasmid pTZAGLYSHR, carrying the hybrid alcohol dehydrogenase-2-glyceraldehyde-3-phosphate dehydrogenase promotor (24) and the chicken lysozyme signal sequence followed by the chemically synthesized human lysozyme gene (18), was constructed starting from pAB24AGScLYSH (16). Plasmid pGEMAGTLYSHR, also derived from pAB24AGScLYSH, carries the promotor, the lysozyme gene, and the glyceraldehyde-3-phosphate dehydrogenase-terminator. It was used as a source of the glyceraldehyde-3-phosphate dehydrogenase-terminator sequence in the final construct.

Plasmid pAB24 is a yeast shuttle vector that contains the entire 2-μm circle needed for replication and the *leu2-d* and *ura3* genes for selection in yeast, as well as the pBR322 sequences necessary for selection and replication in *E. coli* (24).

*Construction of the Chimeric Gene*—The purpose of the present study was to transplant the structural element, which is responsible for the $Ca^{2+}$ binding properties of BLA, into the sterically homologous position in HLY and to study the effects of the newly introduced $Ca^{2+}$ binding capacity on the properties of the hybrid. The transplanted structure is composed of a short $3_{10}$ helix, the $Ca^{2+}$-binding loop, and the central helix C (Fig. 1), and corresponds to the amino acid sequence 72–97 (BLA numbering) (Table I). The construction of the hybrid gene occurred in three steps. In the first, identical restriction sites had to be introduced in register into the plasmids pTZAGLYSHR and pTZs31T, that were used as the source material for the *hly* and *bla* genes, respectively. In the second, the homologous *bla* gene fragment was inserted into the *hly* gene. In the third, the hybrid gene was cloned into the appropriate shuttle vector.

In order to create an *Nde*I site at the position of the *hly* gene corresponding to amino acids 75–77, oligonucleotide-directed mutagenesis according to Kunkel (25) was carried out using the oligonucleotide 5′-CAAGTGACATATGTTAACAGC-3′ as the primer (the *Nde*I site is marked in italics). In order to create an *Xho*II site at codons 101–103 of the lysozyme gene, and to shift the *Xho*II site from the corresponding amino acid position 94–96 to position 96–98 of the α-lactalbumin gene (BLA numbering), we used two oligonucleotides. The first one intended for pTZAGLYSHR was 5′-GATACCTTGTGGATCTAACAACTCT-3′ and the second one for pTZs31T: 5′-GATACGACCGGATCTAGAATCT-TCTTAAC-3′ (the *Xho*II site in both is marked in italics).

By using the newly created *Nde*I restriction site in the *hly* gene and the *Nde*I site already present in the *bla* gene at the corresponding amino acid positions, and both newly created *Xho*II restriction sites in the *hly* and *bla* genes, the *hly* sequence corresponding to the amino acid sequence from Ala-76 to Asp-102 was exchanged for that of *bla*, equivalent to Ile-72 to Asp-97 (BLA numbering). Because the pTZAGLYSHR plasmid contains several *Xho*II sites, it was cut by *Xho*II/*Sal*I and *Sal*I/*Nde*I, respectively. From each digest the appropriate fragment was isolated and ligated to the *Nde*I-*Xho*II fragment of pTZs31T, and the resulting plasmid was named pTZAGLYLA1.

[2] The abbreviations used are: M4, mutant of human lysozyme, obtained by site-directed mutagenesis, in which four (A83K, Q86D, N88D, A92D) residues were changed; HLY, human lysozyme (isolated from milk); BLA, bovine α-lactalbumin; LYLA1, chimera obtained from human lysozyme by substituting the central part for the homologous sequence of bovine α-lactalbumin as described in the text; CAT, chloramphenicol acetyltransferase; $(GlcNAc)_3$ = *N,N′,N″*-triacetylchitotriose; Fura-2, 1-[2-(5′-carboxyoxazol-2′-yl)-6-aminobenzofuran-5-oxy]-2-(2′-amino-5′-methylphenoxy)-ethane-*N,N,N′,N′*-tetraacetic acid; PAGE, polyacrylamide gel electrophoresis.

TABLE I

*Comparison of the amino acid sequences of the chimeric protein LYLA1 and its two parental proteins, human lysozyme and bovine α-lactalbumin*

Bold characters indicate amino acids common to the three proteins. The transplanted BLA part in LYLA1 is underlined. The sequence data for HLY are from Ref. 56 and data for BLA from Ref. 23.

| | | |
|---|---|---|
| HLY | K V F E R **C E L A R T L K** R L G M D **G Y** | 20 |
| LYLA1 | K V F E R **C E L A R T L K** R L G M D **G Y** | 20 |
| BLA | E Q L T K **C E** V F **R E L K** - - D L K **G Y** | 18 |
| HLY | R **G** I **S L** A N **W** M **C** L A K W E **S G Y** N **T** | 40 |
| LYLA1 | R **G** I **S L** A N **W** M **C** L A K W E **S G Y** N **T** | 40 |
| BLA | G **G** V **S L** P E **W** V **C** T T F H T **S G Y** D **T** | 38 |
| HLY | R **A** T N Y **N** A G **D** R **S T** D **Y G** I **F Q I N** | 60 |
| LYLA1 | R **A** T N Y **N** A G **D** R **S T** D **Y G** I **F Q I N** | 60 |
| BLA | Q **A** I V Q **N** - N **D** - **S T** E **Y G** L **F Q I N** | 56 |
| HLY | S R Y **W C** N **D** G K T **P** G A V **N** A **C** H L **S** | 80 |
| LYLA1 | S R Y **W C** N **D** G K T **P** G A V **N** I C N I **S** | 80 |
| BLA | N K I **W C** K **D** D Q N **P** H S S **N** I **C** N I **S** | 76 |
| HLY | **C** S A L **L** Q **D** N I A **D** A V A **C** A **K** R V V | 100 |
| LYLA1 | C D K F L D D D L T D D I M C V K K I L | 100 |
| BLA | **C** D K F **L** D **D** D L T **D** D I M **C** V **K** K I L | 96 |
| HLY | R **D** P Q **G I** R A **W** V **A** W R N R **C** Q N R D | 120 |
| LYLA1 | - D P Q **G I** R A **W** V **A** W R N R **C** Q N R D | 119 |
| BLA | - **D** K V **G I** N Y **W L A** H K A L **C** S E K L | 115 |
| HLY | V R **Q** Y V Q G **C** G - V | 130 |
| LYLA1 | V R **Q** Y V Q G **C** G - V | 129 |
| BLA | D - **Q** W L - - **C** E K L | 123 |

After verifying the sequence of the chimeric *lyla*1 gene, pTZAG-LYLA1 was cut with *Bam*HI and *Sal*I to isolate the DNA sequence corresponding to the promotor, the signal sequence, and the *lyla1* gene. The glyceraldehyde-3-phosphate dehydrogenase-terminator sequence was isolated from pGEMAGTLYSHR as a *Sal*I-*Bam*HI fragment. Both fragments (promotor-signal-gene on the one hand and terminator on the other) were ligated into the *Bam*HI site of pTZ18U to obtain pTZAGLYLA1T. The *Bam*HI-*Bam*HI fragment of the latter, containing the promotor, signal, coding sequence, and terminator, were ligated into the *Bam*HI site of the pAB24 shuttle vector, resulting in the pABAG-LYLA1 expression plasmid.

*Transformation of the Yeast Cells and Expression in Culture Medium*—The newly constructed pABAGLYLA1 was used to transform the *S. cerevisiae* GRF182 strain by the lithium acetate method (26). Uracil-selective medium was used to screen for plasmid-containing cells and $Ura^+$ transformants were grown in leucine-selective medium for 4 days. This culture was used to inoculate (1/20) buffered YPD medium. Cells were grown at 28 °C in shaking culture or in a 10-liter fermentation batch supplied with 4% ethanol after exhaustion of the carbon source. The culture was harvested after 5–7 days of growth.

*Purification*—The LYLA1 protein was purified from the pooled supernatant by repeated cation-exchange and size-exclusion chromatography as follows. The supernatant was diluted with 4 volumes of distilled water and its pH was adjusted to 6.5. It was loaded onto a cation-exchange column Fractogel-$SO_3$ (Merck; type EMD 650 M) which was equilibrated with 20 mM phosphate buffer, pH 6.5. After washing with the same buffer, the chimeric protein was eluted with 1 M NaCl in buffer. Fractions positive for enzymatic or antigenic activity were subjected to size-exclusion chromatography on a Sephacryl HR-100 (Pharmacia) column, using 50 mM NaAc, pH 5.0, 0.2 M NaCl. The fractions containing the chimeric protein were pooled, dialyzed against water, and rerun on the previously mentioned cation exchanger, this time eluted with a linear NaCl gradient (0–1.5 M). The final yield of LYLA1 was between 8 and 9 mg/liter of medium.

The purity of the final product was controlled by sodium dodecyl sulfate-polyacrylamide gel electrophoresis (SDS-PAGE), by isoelectric focusing on precoated plates (Serva) containing an ampholite gradient of pH 3–10, by electrospray-mass spectrometry on a V. G. Biotech BIO-Q instrument, and by N-terminal sequence analysis on a gas phase sequenator (Applied Biosystems model 477A) using Edman chemistry.

*Immunochemical Analysis*—The antigenic properties of the chimeric LYLA1 were analyzed using affinity-purified polyclonal antibodies to the parent proteins BLA and HLY. The latter were prepared by injecting rabbits with recombinant HLY (18) or with natural BLA (21). Antibodies to HLY were affinity-purified on CNBr-activated Sepharose (Pharmacia) to which a commercial preparation of HLY was coupled. Antibodies to BLA were purified as described (21). The presence of antigenic determinants specific for the $Ca^{2+}$-binding loop and the helix C in LYLA1 was confirmed using antibodies induced with a CAT-fusion protein in which the C terminus of CAT was elongated by the BLA sequence 73–105 (16). As both BLA- and HLY-specific epitopes are present on the LYLA1 chimera, measurement of this protein was routinely done with a sandwich immunoradiometric assay (21), using anti-BLA to coat the wells and $^{125}I$-labeled anti-HLY for detection.

*$Ca^{2+}$ Binding Measurements*—The standard enthalpy for $Ca^{2+}$ binding ($\Delta H_{Ca}$) was measured using a batch microcalorimeter (LKB type 2107) (27) and the binding constant ($K_{Ca}$) by competition titration with Fura-2 (14). Decalcification of LYLA1 was performed as described before (28), and the final $Ca^{2+}$ content of the apo form, measured by atomic absorption spectroscopy, was always lower than 0.05 mol/mol of protein.

*Enzymatic Activity*—The lytic activity was measured using *M. luteus* as substrate (29), with the exception that the buffer used was 0.1 M MES, pH 6.2. In order to monitor the effect of $Ca^{2+}$ on the enzymatic activity, the assay mixture was adjusted to either 1 mM $CaCl_2$ or 1 mM EDTA. In a study of the pH dependence of the hydrolytic activity, different buffers were used as indicated. Protein concentrations were determined by absorbance measurements at 280 nm, based on the following values for $A$ (1%): for BLA = 20.1; HLY, A92D, and M4 = 25.5; and LYLA1 = 25.0, computed on the basis of the calculated molecular weight and Tyr and Trp content. Absorbance measurements were done on a Beckman DU-70 spectrophotometer.

The binding of $(GlcNAc)_3$ to these proteins was monitored by the Trp fluorescence enhancement that is induced upon substrate binding to the active site cleft (30). In practice, to 2.0 ml of 0.1 mg/ml protein in 10 mM Tris buffer, pH 7.4, containing either 1 mM $Ca^{2+}$ or 1 mM EDTA, small aliquots of a suitably diluted $(GlcNAc)_3$ solution in water were added. After each addition, the temperature was re-equilibrated to 25 °C and the Trp fluorescence emission spectrum recorded ($\lambda_{exc}$ = 285 nm). The enhanced fluorescence intensity at 325 nm was corrected for dilution and plotted as a function of the logarithm of the total $(GlcNAc)_3$ concentration. From the sigmoidal saturation curves the $pEC_{50}$ (the logarithm of the concentration of $(GlcNAc)_3$ needed to obtain 50% of the maximally enhanced fluorescence intensity) values, that are representative for the relative binding constants, were deduced by the point of inflection. All fluorescence measurements were performed on an Aminco SPF-500 spectrofluorometer, and only corrected spectra are shown.

*Circular Dichroism*—Circular dichroism (CD) measurements were carried out on a Jasco J-600A spectropolarimeter using cuvettes of 1-cm

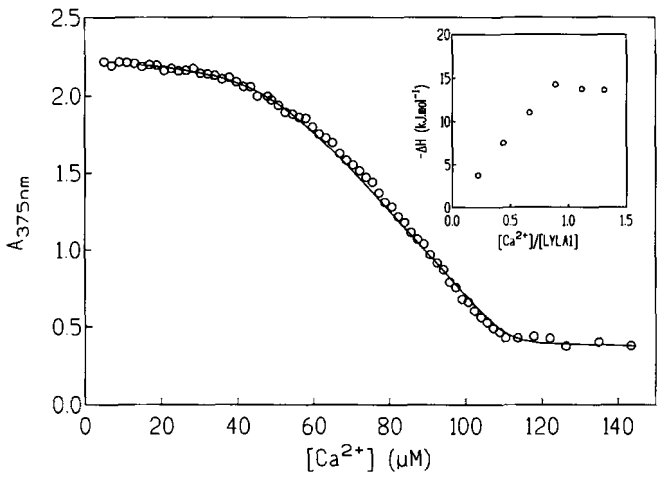


FIG. 2. **Titration of Fura-2 and apoLYLA1 with $Ca^{2+}$.** A mixture of Fura-2 (70.88 μM) and apoLYLA1 (63.43 μM) in 10 mM Hepes, 0.1 M KCl, pH 7.1, was titrated with $Ca^{2+}$ at 20 °C. *Inset*, microcalorimetric titration of apoLYLA1 with $Ca^{2+}$ in 10 mM Tris, pH 7.15, at 25 °C.

path length in the near-UV region and of 1 or 0.1 mm in the far-UV. Base-line normalization was done at 250 (far-UV) and 320 nm (near-UV). The data were expressed as residual ellipticity [$\theta$] (deg·cm$^2$·dmol$^{-1}$) using 115.1 and 113.1 as the mean residue weight for LYLA1 and HLY, respectively.

*NMR Spectroscopy*—NMR spectra were recorded using a GE Omega 500 MHz spectrometer. One-dimensional spectra were measured with a sweep width of 7042 Hz using 4096 points, giving a digital resolution of 1.71 Hz/point. The following two-dimensional experiments were performed for the purposes of assignment and structural analysis: phase-sensitive J-correlated spectroscopy (COSY), single and double relayed coherence transfer spectroscopy, and nuclear Overhauser enhancement spectroscopy (31–33). Data sets were acquired as 512 $t_1$ increments of 2048 data points and 48–96 transients. Several mixing times were used in the nuclear Overhauser enhancement spectroscopy experiment ranging between 150 and 250 ms. Samples were internally referenced using 1,4-dioxane which resonates at 3.743 ppm. All NMR spectra were recorded at pH 4.5, 35 °C, and were processed using the program Felix 2.1 (Hare Research Inc.) on a Sun computer.

*Computer Modeling*—Computer modeling was done on a Silicon Graphics IRIS Indigo computer. The software used for interactive modeling and energy calculations was the BRUGEL program (34). Atomic coordinates used were those of the Brookhaven Protein Data Bank (35) for HLY (code: 1 LZ1) and for baboon α-lactalbumin (code: 1 ALC).

## RESULTS

*Purity Control*—SDS-PAGE of the purified protein indicated that neither aggregation nor fragmentation had occurred (data not shown). On isoelectric focusing, the chimera migrates to a position close to that of HLY. By extrapolation from the reference mixture, the pI of the hybrid is estimated to be 9.6. In comparison with HLY (pI around 11), this figure is consistent with expectations since the hybrid carries four additional Asp residues and one additional Lys. Again, the presence of a single band illustrates the relative purity of the chimera. When measured by electrospray-mass spectrometry, the molecular weight of the peak corresponded to the $Ca^{2+}$ form (14,878 *versus* a predicted value of 14,879). N-terminal sequencing confirmed correct processing by the yeast cells.

*Immunological Properties*—In analogy with previous work on mutant M4 (16), using affinity-purified polyclonal antibodies against the whole BLA molecule and also against a CAT-fusion protein that carries the BLA sequence 73–105, we proved that LYLA1 clearly possesses BLA epitopes (data not shown).

*$Ca^{2+}$ Binding*—The binding of $Ca^{2+}$ to LYLA1 was examined by competition titrations with the $Ca^{2+}$ binding dye, Fura-2 (14) in 0.01 M Hepes, 0.1 M KCl at pH 7.1 and 20 °C. The titration data are consistent with a single, strong binding site with a $K_{Ca}$ of 2.50 (± 0.04) × $10^8$ $M^{-1}$ (Fig. 2). In Table II, thermodynamic data obtained from microcalorimetric titrations are compared with those for BLA, HLY, and the $Ca^{2+}$-binding HLY mutant, M4.

*Enzymatic Activity*—Since the chimera contains the two residues essential for catalytic activity, Glu-35 and Asp-53, one might expect LYLA1 to possess muramidase activity. Also, the introduction of the $Ca^{2+}$ site derived from BLA raises the question whether its lytic activity can be modulated by $Ca^{2+}$ binding. LYLA1 possesses about 10% of the hydrolytic activity of HLY. In the presence of $Ca^{2+}$, the specific activity of HLY (506 enzyme units/mg) is reduced to 46 for LYLA1. In 1 mM EDTA, the corresponding figures are 342 and 53. Thus, the specific activity of the chimera is only slightly dependent on the presence of $Ca^{2+}$.

We also checked the pH dependence of the catalytic activity of LYLA1 and compared it with that of HLY and of its mutant M4 (Fig. 3). The data show that the chimera possesses optimal activity at a pH slightly lower than that of HLY. The figure also indicates the virtual absence of a $Ca^{2+}$ effect at all pH values. In contrast, although no strong $Ca^{2+}$ site has been found on HLY, $Ca^{2+}$ seems to improve its muramidase activity, whereas in the case of the $Ca^{2+}$-binding mutant M4, $Ca^{2+}$ slightly suppresses the catalytic activity.

The binding affinity of the competitive inhibitor $(GlcNAc)_3$ was also evaluated. Binding of this oligosaccharide can conveniently be followed by its enhancing effect on tryptophan fluorescence (30). In Table III the binding data for LYLA1 are compared with those for HLY and its mutant M4. Titrations were performed at two different pH values: 7.4 and 6.0, corresponding to the activity maxima of HLY and LYLA1, respectively. Taken together these data indicate that, first, $(GlcNAc)_3$ binding constants for LYLA1 are 2–3-fold lower than those for HLY and its mutant M4 and, second, that in nearly all cases the presence of $Ca^{2+}$ seems to improve the binding affinity. The slope of the linearized binding curve turns out to be lower for LYLA1 than for the other two proteins (data not shown), suggesting that there is probably more than one binding site for the inhibitor on this hybrid.

Another point of interest is the wavelength of maximal intensity ($\lambda_{max}$) of tryptophan fluorescence and its shift upon saturation with the ligand. The three proteins have a $\lambda_{max}$ of about 330 nm, independent of the presence of $Ca^{2+}$. Upon inhibitor binding, the maximum shows a small blue shift (about 3 nm) in the case of HLY and M4 and a small red shift in the case of LYLA1 (data not shown). More important is the relative increase in quantum yield (Table III). The ratio of the emission intensities measured at saturation with inhibitor *versus* those in its absence ($I_\infty/I_0$) increases in the presence of $Ca^{2+}$ for the three proteins. The difference in the fluorescence increase induced in the different proteins upon saturation with $(GlcNAc)_3$ is large, ranging from 1.9-fold for HLY to 1.3-fold for LYLA1.

*Circular Dichroism*—In order to study the conformational state of the chimeric protein, CD spectra were recorded in the near- and far-UV regions. Fig. 4 shows these spectra for LYLA1 in the presence and absence of $Ca^{2+}$ and compares them with the spectra of wild-type HLY, which are independent of $Ca^{2+}$. The near-UV spectrum of HLY is characterized by a positive band at 292 nm ascribed to tryptophan residues, and a trough near 270 nm, mostly due to tyrosine groups. Apart from intensity differences, especially at 270 nm, these features are also present in the spectrum of the chimera.

In the far-UV region, the spectrum of the apo form of LYLA1 differs markedly from that of wild-type HLY, especially around 190 nm, indicating that the secondary structure of the apo form

TABLE II
*Thermodynamic parameters of $Ca^{2+}$ binding to LYLA1, compared with those for BLA, HLY, and the HLY mutant M4 at 25 °C*

| | $K_{Ca}$ | $\Delta G°$ | $\Delta H°$ | $\Delta S°$ | $-T\Delta S°$ |
|---|---|---|---|---|---|
| | $M^{-1}$ | $kJ\ mol^{-1}$ | | $J\ mol^{-1}\ K^{-1}$ | $kJ\ mol^{-1}$ |
| BLA[a] | $1 \times 10^9$ | $-51 \pm 4$ | $-145 \pm 4$ | $-315 \pm 27$ | $+93 \pm 8$ |
| LYLA1 | $(2.50 \pm 0.04) \times 10^{8b}$ | $-47.91 \pm 0.08$ | $-14 \pm 5$ | $+114 \pm 17$ | $-34 \pm 5$ |
| M4 mutant[a] | $(0.9 \pm 0.05) \times 10^7$ | $-40 \pm 2$ | $-30 \pm 5$ | $+34 \pm 10$ | $-10 \pm 3$ |
| HLY[a] | $(2 \pm 1) \times 10^2$ | $-13 \pm 1$ | $+29 \pm 5$ | $+140 \pm 20$ | $-41 \pm 5$ |

[a] Reported previously (16).
[b] Determined from competition with Fura-2 (14).

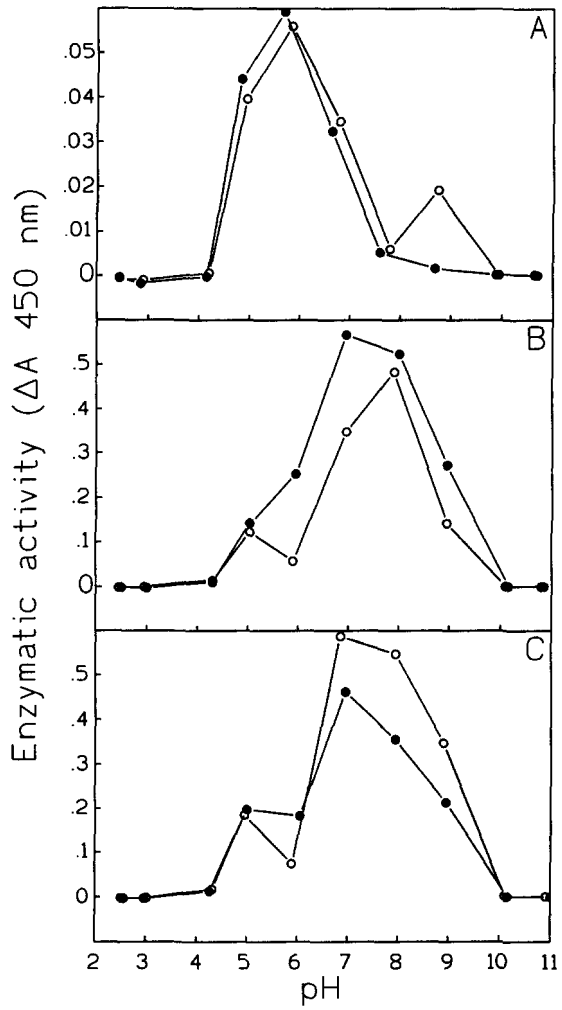


FIG. 3. **Muramidase activity of LYLA1 and HLY toward *M. Luteus*** cell walls at different pH values measured at 25 °C in the presence of 1 mM EDTA (*open symbols*) or 1 mM $Ca^{2+}$ (*filled symbols*). *A*, LYLA1; *B*, HLY; and *C*, HLY mutant M4. Different buffer solutions were used: 50 mM glycine, pH 2–3; 50 mM potassium acetate, pH 4–5; 50 mM MES, pH 6–7; 50 mM Tris, pH 8–9; and 50 mM $KHCO_3$, pH 10–11.

TABLE III
*Binding of $(GlcNAc)_3$ to LYLA1, HLY, and mutant M4 measured from enhancement of tryptophan fluorescence*

Buffers used were either 10 mM Tris-HCl, pH 7.4, or 10 mM MES-KOH, pH 6.0, with addition of either 1 mM $CaCl_2$ or 1 mM EDTA. The logarithm of the $(GlcNAc)_3$ concentration, needed to obtain half-maximal enhancement of fluorescence at 325 nm ($pEC_{50}$), was considered to be a measure of relative binding affinity. Also the ratio of the maximally enhanced *versus* basic fluorescence intensity at 325 nm ($I_\infty/I_0$) was calculated. At pH 6.0, in the presence of EDTA, HLY solutions were slightly opaque, prohibiting spectral measurements.

| | Type | $pEC_{50}$ | | $I_\infty/I_0$ | |
|---|---|---|---|---|---|
| | | $Ca^{2+}$ | EDTA | $Ca^{2+}$ | EDTA |
| pH 7.4 | | | | | |
| | HLY | 4.12 | 3.86 | 1.94 | 1.90 |
| | M4 | 4.57 | 4.16 | 1.57 | 1.40 |
| | LYLA1 | 3.84 | 3.45 | 1.48 | 1.26 |
| pH 6.0 | | | | | |
| | HLY | 4.11 | n.d. | 1.69 | n.d. |
| | M4 | 4.27 | 4.19 | 1.77 | 1.56 |
| | LYLA1 | 3.74 | 3.97 | 1.34 | 1.22 |

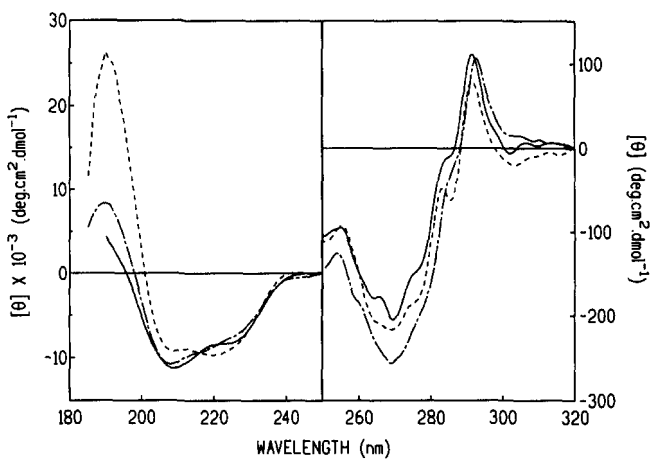


FIG. 4. **CD spectra of LYLA1 at 25 °C in the far- and near-UV.** ——, LYLA1 in 5 mM Tris, 1 mM $Ca^{2+}$, pH 7.55; – – – –, LYLA1 in 5 mM Tris, 1 mM EDTA, pH 7.6; and —·—) recombinant human lysozyme in 5 mM Tris, pH 7.55.

is affected by the presence of the transplanted BLA sequence. In the presence of $Ca^{2+}$ these differences are minimal.

*Tryptophan Fluorescence*—In Fig. 5 the fluorescence emission spectra of LYLA1 measured in the presence and absence of $Ca^{2+}$ are compared with those of natural HLY and BLA. As the spectra for apo- and $Ca^{2+}$-HLY practically coincide, only that of the $Ca^{2+}$ form is shown here. The fluorescence intensity of the chimera is only slightly lower than that observed for HLY. The emission maximum occurs at 328.4 and 327.9 nm for the apo and $Ca^{2+}$ forms of LYLA1, respectively, compared with 330.7 nm for HLY.

No spectral shift and only a small increase in intensity is observed upon $Ca^{2+}$ binding to LYLA1. For BLA by comparison, the binding of $Ca^{2+}$ provokes a large shift in the position of the emission maximum (from 340 to 327 nm) and a significant decrease of fluorescence intensity (36).

*NMR Spectroscopy*—In order to gain information about the secondary and tertiary structure of LYLA1 at the individual residue level, NMR spectroscopy was undertaken. The one-dimensional $^1H$ spectrum of LYLA1 recorded in $D_2O$ is shown in Fig. 6. It is well dispersed and is fully characteristic of a completely folded globular protein (37). The existence of many resolved resonances in the methyl and aromatic regions indicates that the molecule has ordered tertiary structure. Furthermore, in the region between 4.8 and 5.5 ppm several resonances are evident. These arise from C$\alpha$-hydrogens whose downfield shift is indicative of $\beta$-sheet structure. Furthermore, the presence of many amide resonances downfield of 7.0 ppm indicates

that there must be extensive hydrogen-bonded structure, which protects these protons from exchange with the $D_2O$ solvent. Both NMR and electrospray-mass spectrometry show the presence of approximately 55 protected amide hydrogens, very similar to the number found in human lysozyme (38, 39).

In order to analyze the secondary structure of LYLA1 in more detail, two-dimensional NMR methods were employed. Using standard assignment techniques (37) as discussed previously for human lysozyme (38), the main chain resonances of 118 of the 129 residues of LYLA1 were assigned (data available on request). The NOE data were then analyzed to identify the regions of the sequence involved in helical and sheet structure (Table IV). Clear evidence for four $\alpha$ helices was obtained, corresponding closely to helices A–D in the structure of the parent human lysozyme (38, 40). Importantly, the C-helix is clearly evident; this corresponds to a region of the inserted $\alpha$-lactalbumin sequence. The NOE analysis is also indicative of a $\beta$-sheet region between residues 42 and 61, exactly as found in the human protein. Similarly, NOEs characteristic of the $3_{10}$ helices in the parent structure were identified; one of these (residues 121–126) corresponds to a region in the sequence of human lysozyme and one (residues 79–85) to a part of the inserted BLA sequence. Overall, therefore, marked similarity between the secondary structure of LYLA1 and human lysozyme is evident from these data, even in the inserted region.

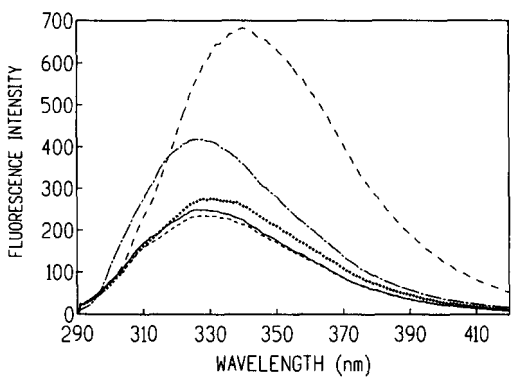


FIG. 5. **Trp fluorescence of LYLA1 at 25 °C.** ——, LYLA1 in 5 mM Tris, 1 mM $Ca^{2+}$, pH 7.5; – – – –, LYLA1 in 5 mM Tris, 1 mM EDTA, pH 7.5; +++, human lysozyme in 5 mM Tris, 1 mM $Ca^{2+}$, pH 7.5; ——, bovine $\alpha$-lactalbumin in 5 mM Tris, 1 mM $Ca^{2+}$, pH 7.5; and — —, bovine $\alpha$-lactalbumin in 5 mM Tris, 1 mM EDTA, pH 7.5.

This conclusion is further supported by analysis of the chemical shift data for the C$\alpha$-H resonances. Residues involved in helices mostly have C$\alpha$-H shifts upfield of the corresponding random coil values, whereas those in $\beta$-sheets are shifted downfield. This approach is simplified in the chemical shift index approach (41) used in Table IV. Comparing the C$\alpha$-H chemical shifts of HLY and LYLA1, not only are the overall patterns identical, but also the individual amplitudes are closely similar (Fig. 7, *A* and *B*). This is particularly true for the first 72 and the last 18 residues (Fig. 7*C*), showing that their environment in nearly all of the HLY-derived part of the chimera is essentially identical to that of the parent HLY. There are two isolated exceptions, Lys-13 and Ala-32. The latter residue is found in the B-helix, very close to the interface with the C-helix of the inserted section. Lys-13 is found on the final turn of the A-helix, and it is this part of the helix which makes contact with the N terminus of the C-helix in the inserted section.

The assignment of the two-dimensional $^1H$ spectrum of LYLA1 has also enabled the regions of structure where backbone amide hydrogens are protected from exchange with solvent hydrogens to be identified. In Fig. 8, the fingerprint region of a two-dimensional COSY spectrum of LYLA1, recorded after the protein was exposed to $D_2O$ at pH 4.5 and 35 °C for several hours, is shown. The resonances in this spectrum arise only from those amide hydrogens whose exchange is slow on the time scale of this experiment and show that amides in all major regions of secondary structure are protected, including at least four of the six helices and both regions of $\beta$-sheet structure. The pattern of protection is broadly consistent with that of human lysozyme (38). Importantly, it includes protection in the substituted region of the sequence, notably in the $3_{10}$ helix (residues 80–85) and the C-helix (residues 90–101) and the region of the sequence where $Ca^{2+}$ binding occurs.

*Thermal Denaturation*—Fig. 9 shows the thermal transition curves of LYLA1 at pH 4.5, measured in the absence (*A*) and in the presence of 10 mM $Ca^{2+}$ (*B*), respectively. In Fig. 10*A*, the same unfolding data are presented in terms of the apparent fractional extent of unfolding ($f_{app}$) *versus* temperature. This fraction was calculated from the ellipticity changes at 270 nm (near-UV) and 222 nm (far-UV) and also from the red shift of

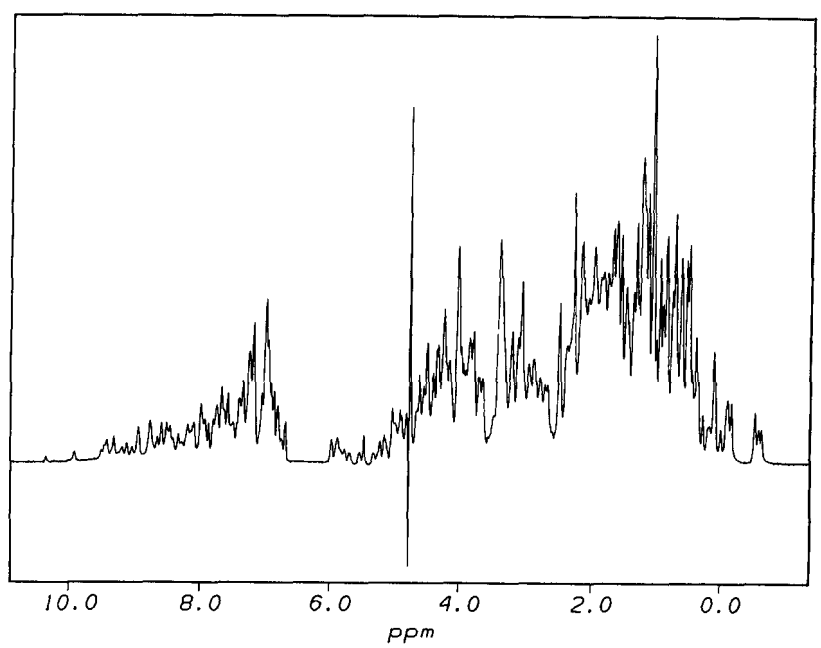


FIG. 6. **One-dimensional $^1H$ NMR spectrum (500 MHz) of LYLA1 in $D_2O$ at 35 °C, pH 4.5.**

TABLE IV
*Secondary structure of LYLA1 derived from chemical shift index analysis (41) and from NOE spectroscopy, compared with HLY (38, 40)*

| Secondary structure element | LYLA1[a] | | HLY |
|---|---|---|---|
| | Residues from CSI | Residues from NOEs | |
| A helix | 7–12 | 4–15 | 4–15 |
| B helix | 26–34 | 26–34 | 24–36 |
| β-sheet | 42–70 | 42–61 | 42–61 |
| $3_{10}$ helix | Not defined | 79–85 | 80–85 |
| C helix | 89–101 | 93–100 | 89–101 |
| D helix | 109–115 | 110–116 | 109–116 |
| $3_{10}$ helix | Not defined | 121–126 | 120–126 |

[a] LYLA1 numbering (*cf.* Table I).

the emission maximum of tryptophan fluorescence upon increasing temperature. In all cases, the transition is fully reversible at this pH. In the presence of 10 mM $Ca^{2+}$, the unfolding curves obtained from CD measurements in the far- and near-UV coincide and indicate a $T_m$ (temperature at the midpoint of a conformational transition) value of 90 °C. Under these conditions, both the secondary (222 nm) and tertiary structure (270 nm) unfold simultaneously in a highly cooperative way.

The thermal unfolding of the apo form of LYLA1, followed by CD at 270 nm and by tryptophan fluorescence, also shows a single cooperative transition, with a $T_m$ of 72.6 °C. Thus, the thermal stability of the chimera is considerably lower in the $Ca^{2+}$-depleted form than in the $Ca^{2+}$-bound form. The unfolding process of the apo form starts at 65 °C and is complete by about 80 °C. In contrast, the transition begins only at 70 °C when followed by CD at 222 nm, resulting in a $T_m$ value of 80.9 °C. Thus, the unfolding of apoLYLA1 does not follow a simple two-state mechanism, but involves population of an intermediate state, since the tertiary structure denatures at lower temperatures than the secondary structure. On the assumption that the residual ellipticity at 222 nm is the same for the native (*N*) and the intermediate (*I*) state, calculations of the fractional amounts of these and of the unfolded (*U*) state were carried out (Fig. 10*A*). These indicate that as much as 65% of the protein is in the I state at 77 °C.

A difference between both $T_m$ values (270 *versus* 222 nm) was also observed in the case of the apo form of M4, a $Ca^{2+}$-binding mutant of HLY (Fig. 10*B*). Here, however, the difference amounts only to 3 °C. In contrast, in the case of HLY, whether $Ca^{2+}$ was present or not, a simple two-state mechanism was found to occur under these conditions, since unfolding measured both at 270 and 228 nm coincides (Fig. 10*C*). The resulting $T_m$ value (78 °C) is far below that of the $Ca^{2+}$ form of LYLA1.

## DISCUSSION

When the degree of structural resemblance between HLY and baboon α-lactalbumin is calculated using the spatial coordinates of the Brookhaven Protein Data Bank (35), a root mean square value of 1.167 Å is obtained for the main chain atoms, indicating a very pronounced three-dimensional homology. Slight deviations are localized in the loop region between residues 62 and 75 and in the region of the C terminus, similar to the differences between HLY and BLA, the latter deduced by homology modeling from the baboon equivalent. This formed the basis for the rationale followed in the present work, *i.e.* to transplant parts of BLA into homologous regions of the HLY molecule and *vice versa* with the aim of obtaining chimeric molecules possessing hybrid functions but with conserved conformations.

One way of building chimeric proteins is by exchanging exons (42–44). Indeed, chicken-type lysozymes and α-lactalbumins might have evolved from a common ancestor through exon shuffling (22, 45). The basic function of lysozyme resides in a single exon (45, 46), which has led Kumagai *et al.* (47) to transplant this exon of hen lysozyme into goat α-lactalbumin. Objections to this rationale (48, 49) are the fact that the complete muramidase function of lysozyme requires residues from different exons and that frequently exon boundaries arise in the middle of secondary structure elements.

The second approach, which is followed here, rests on the exchange of complete secondary structure elements. These are expected to contain sufficient autonomous structural capacity to confer stability to the chimera. Joining of the fused parts

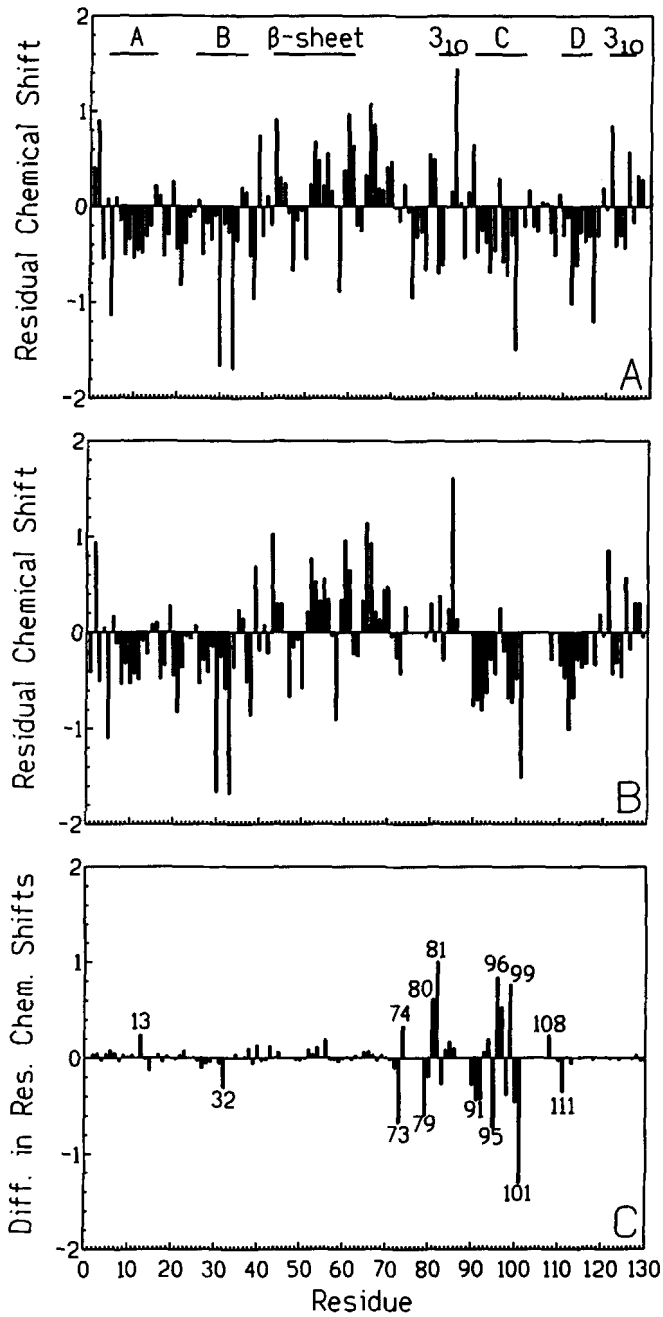


FIG. 7. **Residual Cα-H shift comparison.** Residual chemical shifts are calculated by subtracting the random coil shift (37, 41) from the measured shift. *A*, human lysozyme residual chemical shifts. Elements of secondary structure are indicated. *B*, LYLA1 residual chemical shifts. Residues 75–78 and 87–89 have not been assigned. *C*, difference in residual chemical shift between LYLA1 and HLY. The 15 most perturbed resonances are labeled.

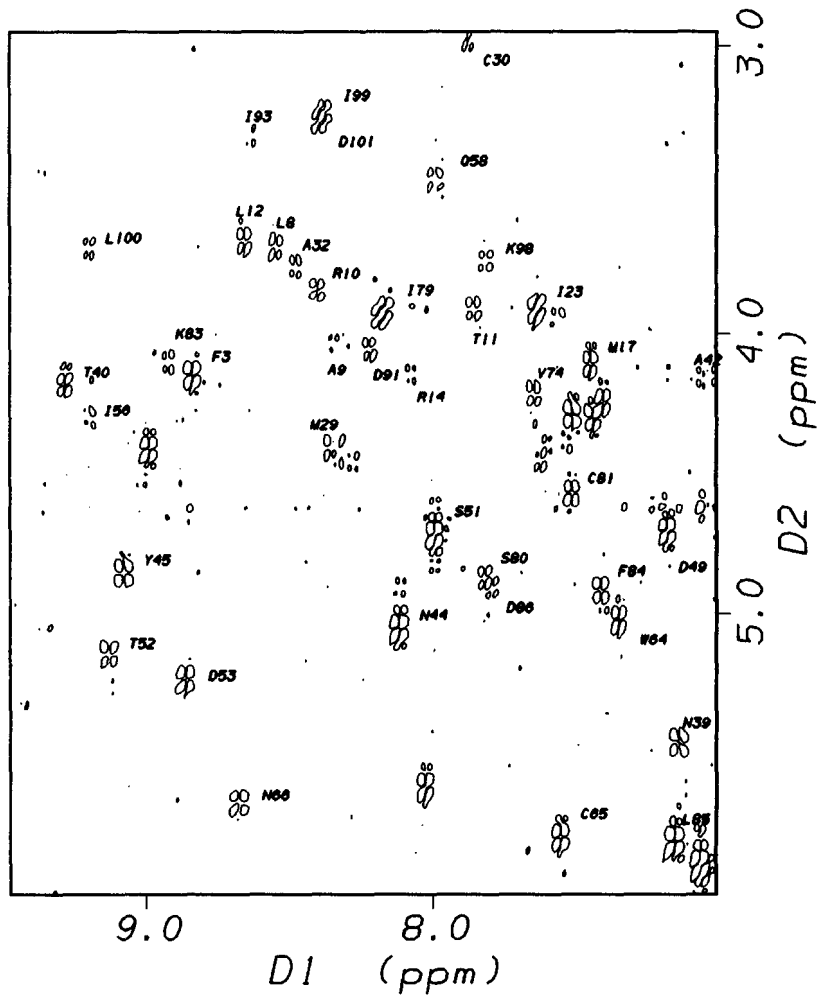


FIG. 8. **500 MHz COSY spectrum of LYLA1 at pH 4.5 and 35 °C showing the fingerprint region where correlations between Cα-H and amide NH protons are observed.** The sample was dissolved 1 h prior to the recording of the spectrum, which took a total of 12 h. The resonances in the spectrum, therefore, all arise from amide hydrogens which are significantly protected from exchange with the $D_2O$ solvent. The amides are largely located in regions of secondary structure in the protein, indicated in Table IV. The prominent peak at 5.61, 8.03 ppm is unassigned but correlates closely with a similar resonance in the COSY spectrum of BLA ( C. M. Dobson, unpublished data); it must therefore arise from the amide of a residue in the inserted region of LYLA1. The unlabeled peak at the *bottom right-hand corner* of the figure is due to aromatic proton correlations.

thus occurs in loops that can adapt to local tensions. Initially, we had planned to introduce into HLY only the BLA sequence needed for a fully equipped $Ca^{2+}$ site. However, as two of the essential aspartate ligands of the $Ca^{2+}$ ion (Asp-87 and Asp-88; BLA numbering) are located on the central α-helix (helix C) adjacent to the $Ca^{2+}$ loop, we finally chose to co-transplant this whole helix together with the authentic BLA-derived $Ca^{2+}$-binding loop and the appending N-terminal arm which contains a 2-turn $3_{10}$-helix.

Compared with the homologous HLY sequence, the transplanted BLA segment shows a deletion at the penultimate position. Consequently, the adjacent Pro-103 is moved one step in the direction of helix C. This could cause the last turn of the transplanted helix to unwind. Nevertheless, by applying the potential function of the BRUGEL software (34) the modeled chimera was indicated to possess sufficient stability. In the contact zone between the HLY and BLA parts a reasonable Van der Waals fit without cavities was observed.

Our two-dimensional NMR analysis confirms these modeling predictions as they show the secondary and tertiary structure of the HLY-derived part of the chimera to be virtually identical to the parent HLY. Also the BLA part of the chimera has a well defined structure related to the native BLA and HLY. This is indicated not only by the NOE and chemical shift data discussed above, but also by the protection from solvent exchange of numerous amide hydrogens. For the region involved, a comparison was made between the differences in residual chemical shifts between LYLA1 and HLY on the one hand (Fig. 7*C*) and between LYLA1 and BLA on the other (data not shown). The latter had to be restricted to helix C as for BLA only a few assignments are available, mostly restricted to this helix (12). This analysis shows that in the second half of the helix (residues 95–101; LYLA1 numbering), there is a much better correlation with the residual shifts of BLA than with those of HLY. The structure of LYLA1 is therefore more likely to be akin to that of BLA in this region, indicating that sequence is more important than micro-environment in determining the local fold. Fig. 11 shows LYLA1 with an indication of the 20 residues possessing the highest residual Cα-H shift differences (Fig. 7*C*). It is immediately obvious that most of them are either part of the substituted region or, when belonging to the HLY part, are in direct contact with this segment. The latter probably experience different packing interactions than when present in the parent HLY. Of particular interest is the subset of residues 98, 99, 100, 101, 108, and 111 (LYLA1 numbering). These residues form a cluster between helices C and D. The former set of four constitutes the last turn of the inserted helix C. In view of the abovementioned single residue deletion, a conformational difference with the homologous turn in HLY is expected.

The hybrid was expressed in substantial amounts in the supernatant of yeast cultures, although yields were markedly lower than for wild-type HLY. This may be due to the presence of the BLA part of the molecule, since we have observed before that using the same promotor recombinant BLA is recovered with a yield of only 1–2 mg/liter (21). In any case, the lower yield of LYLA1 cannot be attributed to a lower stability of the hybrid molecule since in the presence of $Ca^{2+}$ its $T_m$ is even higher than that of the parent HLY. The occurrence of proteolysis can also be ruled out as no fragments were found by

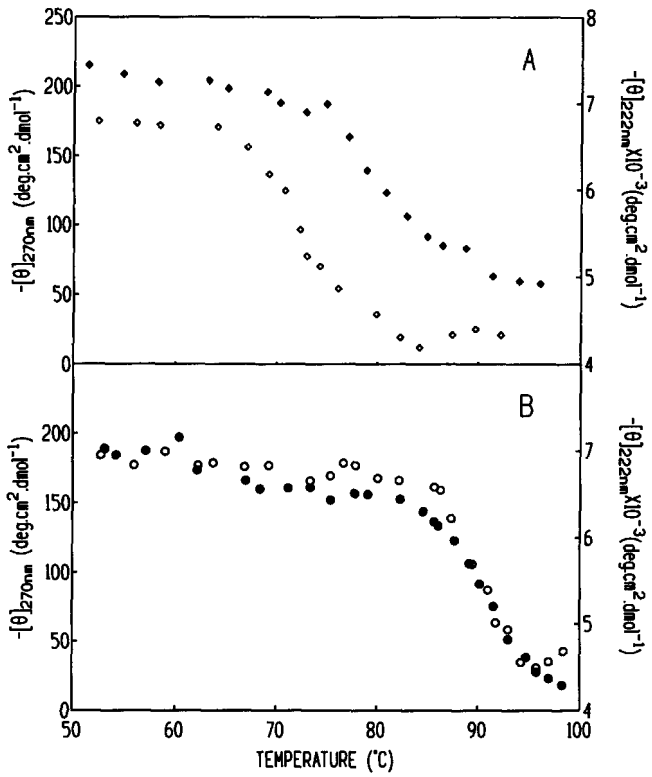


FIG. 9. **Thermal unfolding of apo- and $Ca^{2+}$-LYLA1 followed with CD at 270 nm (*left axes*) and 222 nm (*right axes*).** *A*, residual ellipticity at 270 nm (*open symbols*) and 222 nm (*filled symbols*) for apoLYLA1 in 10 mM NaAc, 90 mM NaCl, pH 4.5; *B*, at 270 nm (*open symbols*) and 222 nm (*filled symbols*) for LYLA1 in 10 mM NaAc, 90 mM NaCl, 10 mM $Ca^{2+}$, pH 4.5.

radioimmunoassay after each chromatographic purification step.

The presence of the $Ca^{2+}$-binding loop was indicated by the pronounced reactivity of the chimera with polyclonal anti-loop antibodies. The binding constant $K_{Ca} = 2.50 (\pm 0.04) \times 10^8\ M^{-1}$ determined by Fura-2 titration, indicates a strong site intermediate in binding strength between that of BLA (27) and the HLY mutant M4 (Table II). Although in the latter all the necessary $Ca^{2+}$ ligands have been introduced, their conformation seems less optimal for binding than in the case of BLA. The fact that the $K_{Ca}$ of BLA is still about four times higher than that of LYLA1 may have to do with the freedom of the former to undergo pronounced conformational changes upon $Ca^{2+}$ binding. Furthermore, $Ca^{2+}$ binding to LYLA1 is characterized by a small negative $\Delta H°$ value and a large positive $\Delta S°$. From similar measurements of $Ca^{2+}$ binding to goat $\alpha$-lactalbumin Desmet *et al.* (50) estimated the fraction of the total $\Delta H°$ and $\Delta S°$ values that is due to "pure" binding, *i.e.* binding not accompanied by conformational changes, to amount to $-36$ ($\pm$ 4) kJ mol$^{-1}$ and +54 ($\pm$ 12) J mol$^{-1}$ K$^{-1}$, respectively. Whereas the thermodynamic data obtained for the M4 mutant come very close to these values, as discussed elsewhere (16), those for LYLA1 are quite different. These deviations could be due to small conformational alterations upon $Ca^{2+}$ binding occurring in the chimera but not in the M4 mutant.

The CD spectrum in the near-UV region of LYLA1 is very similar to that of HLY. Taking into account that the hybrid and the wild-type lysozymes have identical tryptophan and tyrosine residues, these data suggest that the overall tertiary structure of both proteins is very similar. Binding of $Ca^{2+}$ to LYLA1 causes only small changes in conformation as indicated by the CD spectra in both the far- and near-UV range (Fig. 4). By analogy with the CD spectra, virtually no change in the tryptophan fluorescence spectrum is observed upon $Ca^{2+}$ binding (Fig. 5). The spectra of both the apo and the $Ca^{2+}$ form of LYLA1 closely resemble that of HLY, in which exactly the same tryptophan residues are present. Thus, the newly implanted BLA sequence barely affects the fluorescence behavior of these residues. The $\lambda_{max}$ of the emission spectrum is very slightly blue-shifted, indicating that in the hybrid the Trp residues are somewhat more shielded from the solvent than in HLY. In contrast with BLA, upon withdrawal of the $Ca^{2+}$ ion the fluorescence spectrum does not undergo a drastic red shift, indicating that Trp residues do not become more exposed to the solvent.

The chimera also contains both residues essential for the enzymatic activity of lysozyme (Glu-35 and Asp-53) and thus LYLA1 should be an active muramidase. However, hydrolytic activity also implies the correct positioning of the entire active cleft. In LYLA1 most side chains lining the binding cleft are situated in the lysozyme part of the hybrid. The possibility cannot be excluded, however, that the insertion of the $\alpha$-lactalbumin sequence causes small but critical structural changes in the active site region which affect its lytic activity. An indicator of conformational changes that might have occurred in the active cleft is the affinity for inhibitor molecules like $(GlcNAc)_3$. This molecule is able to bind to lysozymes, but it is not susceptible to hydrolysis. In the presence of 1 mM $Ca^{2+}$ at pH 7.4, the chimera shows a rather high relative affinity for $(GlcNAc)_3$ ($pEC_{50} = 3.84$), although this is 2-fold lower than in the case of natural human lysozyme ($pEC_{50} = 4.12$). These data suggest that the active cleft of the chimera is less suitable for $(GlcNAc)_3$ binding than that of human lysozyme. It has already been pointed out from NMR analysis that residues 98–101 (LYLA1 numbering) show conformational or environmental differences compared to the equivalent HLY residues. Also, as discussed above the deletion of a single residue at the C-terminal end of helix C could cause the two subsequent residues to adopt a BLA-like conformation. This region is likely to constitute part of the $(GlcNAc)_3$ binding site if binding can be conceived to occur as in HLY. Therefore, these considerations can also, at least partially, explain the reduced lytic activity toward bacterial cell walls.

One of the most obvious manifestations of $Ca^{2+}$ binding is its effect on the thermal stability of the chimera. Upon increasing the temperature, the $Ca^{2+}$ form denatures cooperatively according to a simple two-state mechanism as is the case for wild type human lysozyme under similar conditions. The observed $T_m$ is even higher than that of HLY. The unfolding of apoLYLA1 at pH 4.5, however, followed by ellipticity measurements at 222 and 270 nm, respectively, does not obey a simple two-state mechanism involving only the native (N) and the fully denatured state (U). The noncoincidence of both unfolding curves can be explained assuming a three-state unfolding mechanism with a partially unfolded intermediate state (I), referred to as a "molten globule" state. In the temperature zone from 65 to 90 °C a fraction ($f_I$) of the chimera is present in the intermediate state (Fig. 10*A*). Similarly, for BLA a molten globule state is found under various experimental conditions (51–53). Up to now no such intermediate state has been reported for HLY under such conditions, although we recently found evidence for a partially folded state at very low pH (17). Therefore, it is extremely interesting to note that in the hybrid, LYLA1, the capacity to form a molten globule state at pH 4.5 has been transferred together with the implantation of a restricted part of BLA. Apparently this part of the molecule is a key element for molten globule formation. Recently it was shown that the helical domain of human $\alpha$-lactalbumin in isolation forms a molten globule with the same

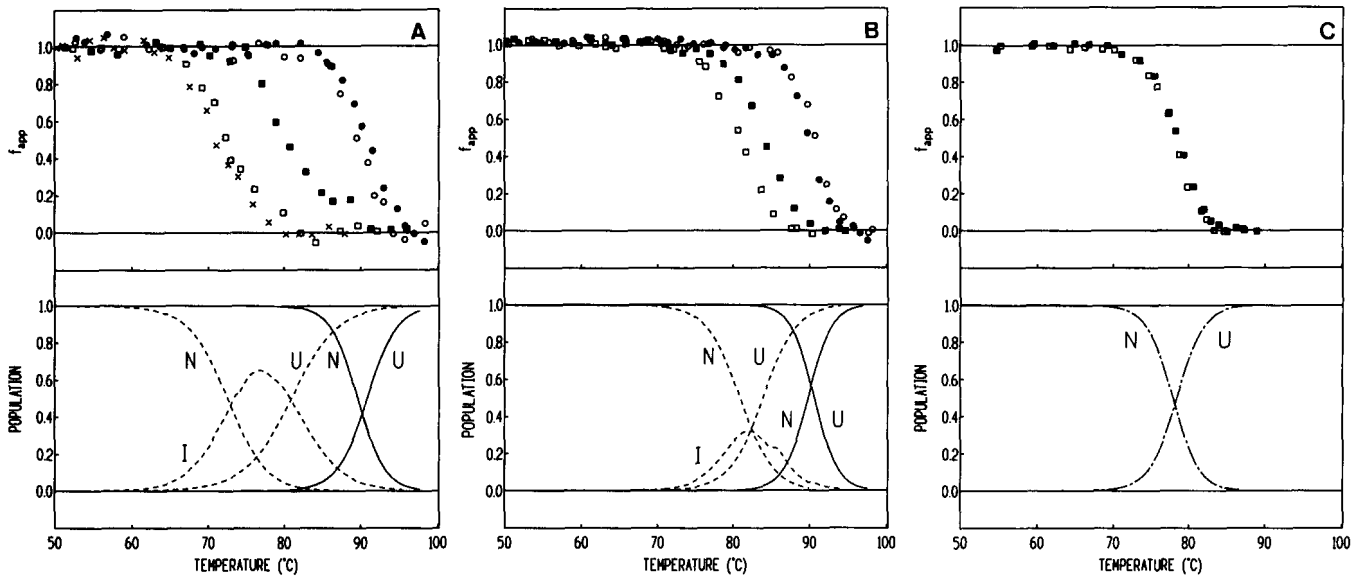


FIG. 10. **Thermal unfolding of LYLA1 (*A*), mutant M4 (*B*), and HLY (*C*) in the presence or absence of $Ca^{2+}$.** *Upper part*, apparent fractions were calculated from residual ellipticities measured for the apo forms (*squares*) in 10 mM NaAc, 90 mM NaCl, pH 4.5, for the $Ca^{2+}$ forms (*circles*) in the same buffer with 10 mM $Ca^{2+}$ added. In the case of HLY, only the data in the absence of $Ca^{2+}$ were shown as they coincide with those in the presence of $Ca^{2+}$. Residual ellipticities were measured in the near-UV at 270 nm (*open symbols*) and in the far-UV at 222 nm (*filled symbols*) or at 228 nm in the case of HLY. Thermal unfolding of apoLYLA1 was also followed by tryptophan fluorescence (*crosses*) measured as the ratio of emission intensities $I_{315}$ nm/$I_{345}$ nm. *Lower part*, population of the N, I, and U states is shown for the apo (*dashed lines*) and the $Ca^{2+}$ forms (*full lines*), respectively.

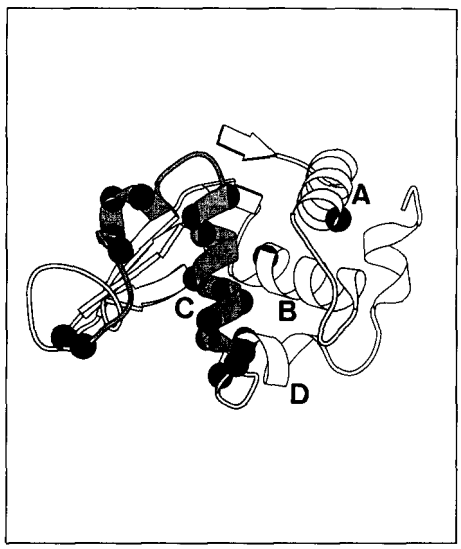


FIG. 11. **Position of the Cα-H resonances showing the largest differences in residual chemical shift between LYLA1 and HLY.** The *gray shaded area* represents the inserted BLA sequence, *filled circles* represent the position of the α carbons with a difference in residual chemical shift of >0.2 ppm. This figure was produced using Molscript software (55).

overall fold of the intact molecule (54). Nevertheless, with the present work the question remains whether it is the $Ca^{2+}$-binding loop or helix C that determines this character. On the one hand, the apo form of the $Ca^{2+}$-binding mutant M4 (16) shows an intermediate state during thermal denaturation at pH 4.5 (Fig. 10*B*). This suggests that the peculiar aspartate-rich sequence of the $Ca^{2+}$ site is at least one of the contributions to the stability of the molten globule state. In accord with this we have described the existence of an intermediate state for the apo form of the $Ca^{2+}$-binding equine lysozyme (13). On the other hand, the fractional population of intermediate state molecules is very limited in M4, amounting only to a maximum of about 32%, compared with 65% in LYLA1. This suggests that helix C of the BLA molecule itself carries important features that determine molten globule propensity. In accord with this conclusion, this helix has been found to have a high level of persistence within the molten globule state of α-lactalbumins (12).

In conclusion, by transplanting the $Ca^{2+}$-binding loop and helix C of BLA we have been able to introduce into HLY one of the most striking properties of BLA, *i.e.* the ability to form a stable molten globule state under relatively mild conditions. By optimization of the length of the transplanted BLA segment we hope to define further the structural basis for this interesting characteristic of α-lactalbumins and hence to understand the factors stabilizing intermediate states of proteins in general.

*Acknowledgments*—We thank Dr. Carol Robinson and Gary Howarth for analysis of LYLA1 by electrospray mass spectroscopy, Dr. Lorna Smith for advice on structural analysis by NMR spectroscopy, and Dr. Christina Redfield and Christopher Penkett for valuable discussions. The expert technical assistance of Sigried Vanryckeghem, Linda Desender, Hilde Verhaeghe, Wim Noppe, and Frederik Coornaert is gratefully acknowledged.

REFERENCES

1. Nitta, K. & Sugai, S. (1989) *Eur. J. Biochem.* **182,** 111–118
2. Kuwajima, K., Hiraoka, Y., Ikeguchi, M. & Sugai, S. (1985) *Biochemistry* **24,** 874–881
3. Ikeguchi, M., Kuwajima, K., Mitani, M. & Sugai, S. (1986) *Biochemistry* **25,** 6965–6972
4. Dobson, C. M. (1991) *CIBA Found. Symp.* **161,** 167–189
5. Brew, K., Vanaman, T. C. & Hill, R. L. (1967) *J. Biol. Chem.* **242,** 3747–3749
6. Smith, S. G., Lewis, M., Aschaffenburg, R., Fenna, R. E., Wilson, I. A., Sundaralingam, S. D. I., Stuart, D. I. & Phillips, D. C. (1987) *Biochem. J.* **342,** 353–360
7. Acharya, K. R., Stuart, D. I., Walker, N. P. C., Lewis, M. & Phillips, D. C. (1989) *J. Mol. Biol.* **208,** 99–127
8. Stuart, D. I., Acharya, K. R., Walker, N. P. C., Smith, S. G., Lewis, M. & Phillips, D. C. (1986) *Nature* **324,** 84–87
9. Dolgikh, D. A., Gilmanshin, R. I., Brazhnikov, E. V., Bychkova, V. E., Semisotnov, G. V., Venyaminov, S. Y. & Ptitsyn, O. B. (1981) *FEBS Lett.* **136,** 311–315
10. Kuwajima, K. (1989) *Proteins Struct. Funct. Genet.* **6,** 87–103
11. Haynie, D. T. & Freire, E. (1993) *Proteins Struct. Funct. Genet.* **16,** 115–140
12. Alexandrescu, A. T., Evans, P. A., Pitkeathly, M., Baum, J. & Dobson, C. M. (1993) *Biochemistry* **32,** 1707–1718
13. Van Dael, H., Haezebrouck, P., Morozova, L., Arico-Muendel, C. & Dobson, C. M. (1993) *Biochemistry* **32,** 11886–11894
14. Nitta, K., Tsuge, H., Shimazaki, K. & Sugai, S. (1988) *Biol. Chem. Hoppe-Seyler* **369,** 671–675

15. Kuroki, R., Taniyama, Y., Seko, C., Nakamura, H., Kikuchi, M. & Ikehara, M. (1989) *Proc. Natl. Acad. Sci. U. S. A.* **86,** 6903–6907
16. Haezebrouck, P., De Baetselier, A., Joniau, M., Van Dael, H., Rosenberg, S. & Hanssens, I. (1993) *Protein Eng.* **6,** 643–649
17. Haezebrouck, P., Joniau, M., Van Dael, H., Hooke, S. D., Woodruff, N. D. & Dobson, C. M. (1995) *J. Mol. Biol.* **246,** 382–387
18. De Baetselier, A., Rosenberg, S. & Hanotier, J. (1989) European Patent Application 89870140.4
19. Malcolm, B. A., Rosenberg, S., Corey, M. J., Allen, J. S., De Baetselier, A. & Kirsch, J. F. (1989) *Proc. Natl. Acad. Sci. U. S. A.* **86,** 133–137
20. Erhart, E. & Hollenberg, C. P. (1983) *J. Bacteriol.* **156,** 625–635
21. Viaene, A., Volckaert, G., Joniau, M., De Baetselier, A. & Van Cauwelaert, F. (1991) *Eur. J. Biochem.* **202,** 471–477
22. Vilotte, J. L., Soulier, S., Mercier, J. C., Gaye, P., Hue-Delahaie, D. & Furet, J. P. (1987) *Biochimie (Paris)* **69,** 609–620
23. Shewale, J. G., Sinha, S. K. & Brew, K. (1984) *J. Biol. Chem.* **259,** 4947–4956
24. Barr, P. J., Gibson, H. L., Enea, V., Arnot, D. E., Hollingdale, M. R. & Nussenzweig, V. (1987) *J. Exp. Med.* **165,** 1160–1171
25. Kunkel, T. A. (1985) *Proc. Natl. Acad. Sci. U. S. A.* **81,** 4642–4646
26. Elble, R. (1992) *BioTechniques* **13,** 18–20
27. Desmet, J., Hanssens, I. & Van Cauwelaert, F. (1987) *Biochim. Biophys. Acta* **912,** 211–219
28. Haezebrouck, P., Noppe, W., Van Dael, H. & Hanssens, I. (1992) *Biochim. Biophys. Acta* **1122,** 305–310
29. Kikuchi, M., Yamamoto, Y., Taniyama, Y., Ishimaru, K., Yashikawa, W., Yoshihiko, K. & Ikehara, M. (1982) *Proc. Natl. Acad. Sci. U. S. A.* **85,** 9411–9415
30. Chipman, D., Grisaro, V. & Sharon, N. (1967) *J. Biol. Chem.* **242,** 4388–4394
31. Jeener, J., Meier, B. H., Bachmann, P. & Ernst, R. R. (1979) *J. Chem. Phys.* **71,** 4546–4553
32. Kumar, A., Ernst, R. R. & Wüthrich, K. (1980) *Biochem. Biophys. Res. Commun.* **95,** 1–6
33. Macura, S., Huang, Y., Suter, D. & Ernst, R. R. (1981) *J. Magn. Reson.* **43,** 259–281
34. Delhaise, P., Bardiaux, M. & Wodak, S. (1984) *J. Mol. Graph.* **2,** 103–106
35. Bernstein, F. C., Koetzle, T. F., Williams, G. J., Meyer, E. E. Jr., Brice, M. D., Rodgers, J. R., Kennard, O., Shimanouchi, T. & Tasumi, M. (1977) *J. Mol. Biol.* **112,** 535–542
36. Murakami, K., Andree, P. J. & Berliner, L. J. (1982) *Biochemistry* **21,** 5488–5494
37. Wüthrich, K. (1986) *NMR of Proteins and Nucleic Acids,* Wiley, New York
38. Redfield, C. & Dobson, C. M. (1990) *Biochemistry* **29,** 7201–7214
39. Hooke, S. D., Radford, S. E. & Dobson, C. M. (1994) *Biochemistry* **33,** 5867–5876
40. Artymiuk, P. J. & Blake, C. C. F. (1981) *J. Mol. Biol.* **152,** 737–762
41. Wishart, D. S., Sykes, B. D. & Richards, F. M. (1992) *Biochemistry* **31,** 1647–1651
42. Gilbert, W. (1978) *Nature* **271,** 501
43. Blake, C. C. F., (1979) *Nature* **277,** 598
44. Go, M. (1983) *Proc. Natl. Acad. Sci. U. S. A.* **80,** 1964–1968
45. Jung, A., Sippel, A. E., Grez, M. & Schütz, G. (1980) *Proc. Natl. Acad. Sci. U. S. A.* **77,** 5759–5763
46. Kuchinke, W. (1989) *Biochem. Biophys. Res. Commun.* **159,** 927–932
47. Kumagai, I., Takeda, S. & Miura, K.-I. (1992) *Proc. Natl. Acad. Sci. U. S. A.* **89,** 5887–5891
48. Traut, T. W. (1988) *Proc. Natl. Acad. Sci. U. S. A.* **85,** 2944–2948
49. Stoltzfus, A., Spencer, D. F., Zuker, M., Logsdon, J. M., Jr. & Doolittle, W. F. (1994) *Science* **265,** 202–207
50. Desmet, J., Tieghem, E., Van Dael, H. & Van Cauwelaert, F. (1991) *Eur. Biophys. J.* **20,** 263–268
51. Kronman, M. J. (1989) *Crit. Rev. Biochem. Mol. Biol.* **24,** 565–667
52. Segawa, T. & Sugai, S. (1983) *J. Biochem. (Tokyo)* **93,** 1321–1328
53. Ikeguchi, M., Kuwajima, K. & Sugai, S. (1986) *J. Biochem. (Tokyo)* **99,** 1191–1201
54. Peng, Z. & Kim, P. S. (1994) *Biochemistry* **33,** 2136–2141
55. Kraulis, P. (1991) *J. Appl. Crystallogr.* **24,** 946–950
56. Canfield, R. E., Kammerman, S., Sobel, J. H. & Morgan, F. J. (1971) *Nature New Biol.* **232,** 16–17